A FEASIBLE LOSS MODEL FOR IGBT

Marcelo C. Cavalcanti[1], Edison R. da Silva[2], Dushan Boroyevich[3], Wei Dong[3], and Cursino B. Jacobina[2]

[1]Departamento de Engenharia Elétrica e Sistemas de Potência, Universidade Federal de Pernambuco
Recife, PE, Brasil, Tel. +55 (81) 3271-8255
marcelo.cavalcanti@ufpe.br

[2]Departamento de Engenharia Elétrica, Universidade Federal de Campina Grande
Campina Grande, PB, Brazil, Tel. +55 (83) 310-1407
edison,jacobina@dee.ufcg.edu.br

[3]Center for Power Electronics Systems, Virginia Polytechnique Institute and State University
Blacksburg, VA, USA, Tel . +1 (703) 231-4536
dushan,wedong@vt.edu

***Abstract* — This paper proposes an efficient loss model to estimate IGBT losses at operating points not given in data sheets. It investigates power losses of IGBT as a function of the circuit its and operating parameters in order to help the device selection for a given application. Loss models for hard switching and soft switching are developed based on experimental determination of the power losses.**

KEYWORDS

IGBT, loss model, conduction loss, switching loss.

I. INTRODUCTION

IGBT is among the most used power semiconductor devices in power electronics applications. Although IGBT's have improved dramatically in terms of their conduction and switching losses [1], management of these power losses remains as a key issue in IGBT based power converters design. The device selection often involves a trade-off between fast switching characteristics (i.e., lower switching losses) and lower on-state conduction losses. In addition, many other parameters that affect the device losses must be considered, such as gate drive circuit parameters, temperature, and switching pattern. It is obviously very important for the converter designer to have good models for loss estimation. Data sheets from devices usually have limited data for limited operating conditions and fixed parameters. It is the device user's task to come up with a loss model that applies to the actual operating conditions.

Usually, two different types of equations are used to represent losses in IGBT: power equations [2] or linear equations [3,4]. These equations can be used, for instance, to estimate losses in a PWM voltage source inverter. But the results only compare PWM methods and it is not clear which type of equation is the best approximation to reproduce IGBT losses. On the other hand, equations can be developed to estimate losses produced by specific PWM strategies in hard [3] and soft-switching inverters [5]. In addition, not always the conditions of operation coincide with those given in the restrict data sheets (different current, temperature, gate drive resistance). In these cases it is possible to calculate the device conduction and switching losses by generating the necessary information from tabular information together with interpolation of graphs in data sheets and the knowledge of the current waveform. This is also possible with the use of model parameters derived from tables. Unfortunately, in most design problems the temperature junction is unknown and fixed temperature parameters is not useful. A linear regression is then done. The case is more complex when the IGBT operates under different soft switching conditions in different applications (hard-switching, HS, zero-voltage-switching, ZVS, zero-current-switching, ZCS, and zero-voltage-zero-current switching, ZVZCS) [6]-[8]. One possibility is to measure losses directly in the power converter assembly. But besides the difficulties due to the resolution for precise measurement and the influence of parasites or additional components, this becomes a hard task when the efficiency of a large number of topologies is to be compared. These problems can be overcome by deriving the model parameters from measurement since they are more accurate than those obtained from linear regression [2]. This can be done from basic test circuits in which the device is tested under different conditions. An alternative to this is to simulate the test circuit in SPICE using the SPICE models of the device.

The approach investigated in this paper allows the optimal choice of IGBT's for any application using loss models that take into account several variables in a same equation. The energy loss models are obtained from tables built from experimental results and a curve fitting technique. The use of mathematical models based on polynomial equations of second order obtained from experimental tests are compared to those obtained with the use of IGBT SPICE models and to those obtained from the use of equations of first order. The

proposed selection method is not restricted to IGBT's, but can also be employed with other power semiconductors.

II. DESCRIPTION OF THE LOSS MODEL

This section presents the methodology that allows comparing losses of converters by simulation. In the methodology presented here for the study of losses, the physics of the devices is not included in the models. However, mathematical models are used to represent the behavior of the devices at the required situations.

A. Conduction losses

The conduction energy losses in an IGBT or a diode can be expressed as

$$E_C = \int_0^{t_C} U_C(I) I(t) dt \qquad (1)$$

where E_c is the conduction energy, U_c is the conduction voltage or collector-emitter on-state voltage drop, I is the collector current, and t_c is the conduction time. The conduction voltage is a function of current and temperature. At a given temperature, the relationship between U_c and I is generally nonlinear but usually characterized by a linear equation. Although a linear approximation is often used, a second order polynomial equation is a better characterization of the conduction voltage. The general relation for the polynomial equation is

$$U_C = a_C + b_C \cdot I + c_C \cdot I^2 \qquad (2)$$

where a_c, b_c, c_c are coefficients from curve fitting of data provided from the device data sheets or test data. It is important to use a test circuit to characterize the device because different operating points can be measured, allowing the inclusion of different parameters in the loss models.

The curves in Fig. 1 compare the voltage drop of IGBT CM150DY-24H as obtained from experimental data, from simulation of the test circuit using the IGBT SPICE model, and from data sheet for temperatures usually given in data sheet. Note that for a temperature of 25°C the three curves converge. However, for 125°C the results obtained with SPICE (model for 25°C) and from data sheet diverge, with an error of 20% in some of the points.

In order to consider the temperature effects, the conduction losses equation needs to have more terms and a better approximation can be obtained by using a power equation, that is,

$$U_C = a_C \cdot T^{at} + b_C \cdot T^{bt} \cdot I + c_C \cdot T^{ct} \cdot I^2 \qquad (3)$$

Table I shows the comparison of experimental data with the estimated conduction losses by the use of equation (3) at

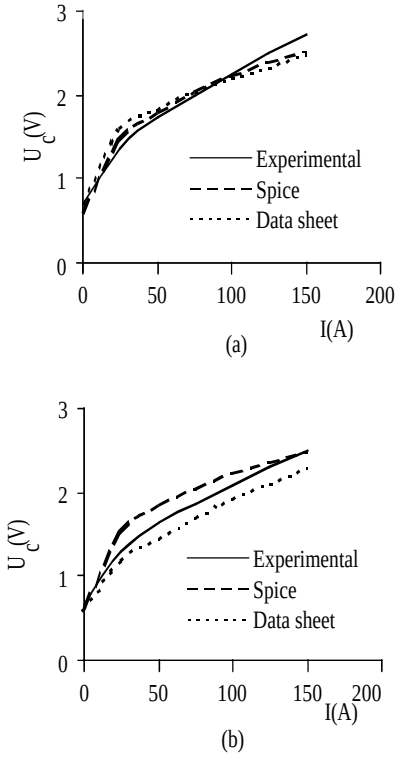

Fig.1. Characteristics of conduction (IGBT CM150DY-24H): (a) T = 25°C; (b) T = 125° C

different current and temperature conditions for a given IGBT. In the table, the conduction voltage is shown for three different temperatures (25°C, 75°C and 125°C). The small errors obtained confirm the validity of the model.

B. Switching losses

Switching losses can be characterized similarly to the conduction losses but instead more variables must be included. In addition to current and temperature, hard switching losses are function of the dc voltage and gate drive resistance. Also the diode reverse recovery is an integral part of the switching process and affects the overall losses. Turn-on and turn-off losses must also be considered in separate. A second order polynomial will be used here because results are more accurate when compared to other approximations.

Switching losses in an IGBT or a diode can be expressed

TABLE I
Comparison of the conduction voltage model for three different temperatures

	I (A)	0	50	100	150
Uc (V)	Experim	0.77	1.69	2.33	2.70
T=25°C	Equation	0.78	1.70	2.35	2.72
Uc (V)	Experim	0.76	1.64	2.25	2.58
T=75°C	Equation	0.76	1.63	2.23	2.55
Uc (V)	Experim	0.73	1.58	2.15	2.45
T=125°C	Equation	0.75	1.60	2.17	2.47

as

$$E_{sw} = a_i \cdot T^{at} \cdot E^{av} \cdot R^{ar} + b_i \cdot T^{bt} \cdot E^{bv} \cdot R^{br} \cdot I + c_i \cdot T^{ct} \cdot E^{cv} \cdot R^{cr} \cdot I^2 \quad (4)$$

where E_{sw} is the switching energy, E is the voltage across the switch and R is the gate drive resistance.

Figures 2(a) and 2(b) show the curve fitting results for turn-off and turn-on energy, respectively, for different temperatures and voltages. In these figures the energy estimated from equation (4) is compared to experimental results.

From waveforms obtained with the test circuit, the switching energy losses as a polynomial equation for operation of IGBT CM150DY-24 under ZVS is a function of current and capacitance and is expressed as

$$E_{sw} = 3.1 \cdot C_r^{0.7} + 0.02 \cdot C_r^{-0.1} \cdot I + 6.2 \cdot 10^{-4} \cdot C_r^{-1.03} \cdot I^2$$

(at turn-off), (5)

and

$$E_{sw} = 0.9 \cdot C_r^{0.6} + 0.05 \cdot C_r^{-0.9} \cdot I + 9.2 \cdot 10^{-5} \cdot C_r^{-1} \cdot I^2$$

(at turn-on) (6)

These losses are compared to the experimental ones in Fig. 3.

Similar equations, but as function of inductance and voltage, are presented for ZCS as

$$E_{sw} = 0.06 \cdot L_r^{-0.5} + 0.001 \cdot L_r^{-1.2} \cdot E + 2 \cdot 10^{-6} \cdot L_r^{0} \cdot E^2$$

(at turn-off), (7)

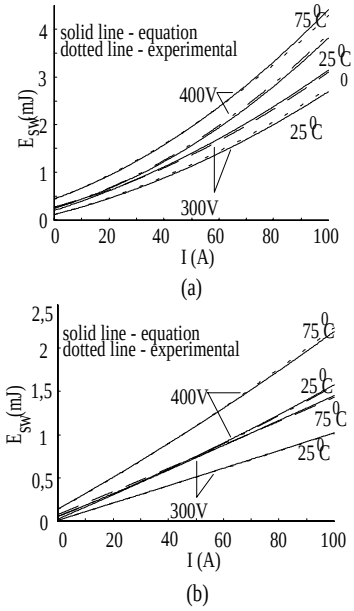

Fig.2 Energy losses for IGBT CM150DY-24H IGBT under HS and different voltages and temperatures: (a) turn-off and (b) turn-on

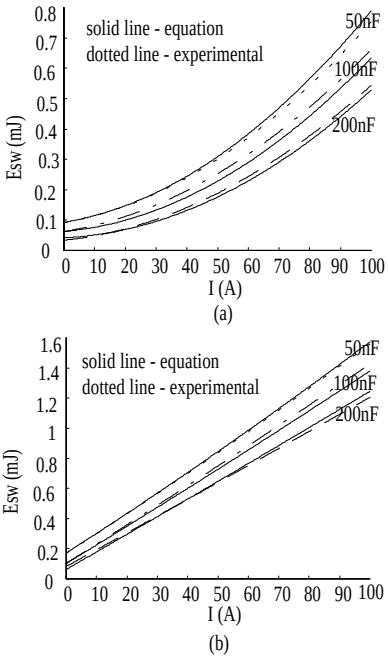

Fig.3. Energy losses versus C_r for an IGBT under ZVS condition: (a) turn-on and (b) turn-off

and

$$E_{sw} = 0.27 \cdot L^{-0.4} + 0.0008 \cdot L^{-0.55} \cdot E + 2 \cdot 10^{-6} \cdot L^{0} \cdot E^2$$

(at turn-on) (8)

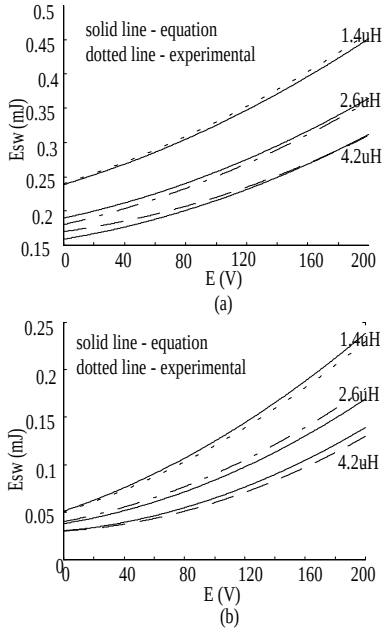

Fig.4. Energy losses versus L_r for an IGBT under ZCS condition: (a) turn-on and (b) turn-off

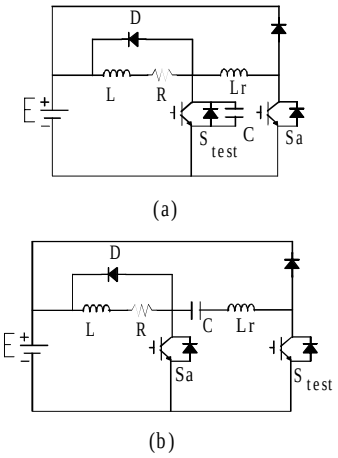

Fig.5. Experimental circuits to test (a) ZVS and (b) ZCS operation

The switching energy losses are compared to the experimental ones in Fig. 4, for turn-on and turn-off.

The waveforms obtained from the test circuits (Fig. 5) are shown in Fig. 6 and Fig. 7 for ZVS and ZCS conditions, respectively.

The loss models obtained are then introduced in a simulation program to evaluate losses of any converter under any operating condition. Two application examples will be discussed next.

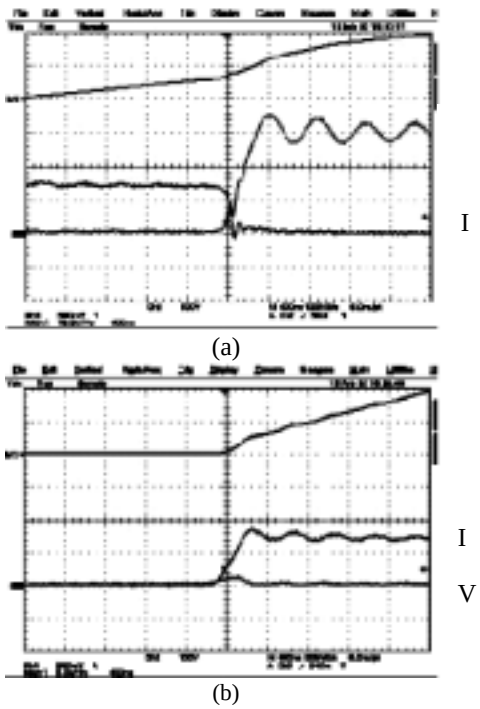

Fig.6. Experimental results for an IGBT under ZVS condition: (a) turn-off and (b) turn-on. Loss energy (top); voltage (100V/div.); and current (50A/div.)

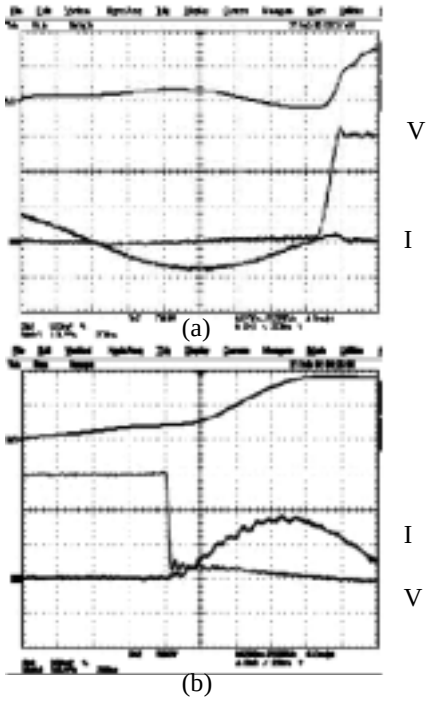

Fig.7. Experimental results for an IGBT under ZCS condition: (a) turn-off and (b) turn-on. Loss energy (top); voltage (50V/div.); and current (50A/div.)

III. APPLICATION EXAMPLES

The method described in section II was applied in two different cases.

A. Example 1

Space Vector Modulation (SVM) is nowadays the PWM technique most used to control hard and soft-switched inverters. SVM is based on the concept of approximating a rotating reference voltage space vector with those realizable on a three-phase inverter, that is, six possible switching states plus two free wheeling states of the inverter. An optimal pulse width modulation is obtained on a volt-second average basis if only the three switching states adjacent to the reference vector are used [9]. In this case each phase is switched in sequence in such a way that switching only one inverter leg performs the transition from one state to the next. A possibility to reduce the number of switching is the Two-Phase Modulation in which only two phases are modulated while the third phase is clamped to the positive or negative DC rail. Since clamping implies in no switching losses, such technique reduces losses in each switching period.

The method in section II was applied in the case of design of an IGBT-based three-phase PWM voltage source inverter. Table 2 shows the average power losses for a 4kW inverter. Four different PWM techniques were tested: sinusoidal PWM (SPWM), continuous PWM (CPWM) and two discontinuous PWM (DPWM) techniques. DPWM1 always use the bottom

switches for freewheeling while DPWM2 always uses top switches for freewheeling. Simulation using the proposed equations and experimental results are shown in the table.

The modulation index was defined as

$$m = 2V_{ab}/\sqrt{3}E \quad (9)$$

where V_{ab} is the amplitude of the line voltage and E is the DC link voltage. The m index assumes values between 0 and $2/\sqrt{3}$. For m = 1, the inverter output rms voltage is 173.2V.

In table II the maximum error between experimental results and simulated results using the proposed equations is about 1.5%. So the model results are in the acceptable range because errors are small and the equipment used to do the tests has 2% tolerance error. The worst case occurred for DPWM2. The advantage of having a better estimation for losses is reflected on the junction temperature and consequently on the thermal design. The main advantage of using simulation combined with the proposed equations is that it is possible include the real temperature in the device. Considering the thermal resistance for the IGBT and diode, the junction temperature can be estimated and the losses can be considered for that value. The use of a good model improves the thermal design that is one of most expensive parts in a project.

B. Example 2

The Quasi-Square-Wave (QSW) voltage converters use ZVS, ZCS, or simultaneous application of ZVS and ZCS conditions. In addition, it has already been shown that the harmonic content in QSW inverters is not too far from that of the conventional schemes. In these circuits, the DC-link voltage is shaped by a single auxiliary wave shaping circuit so that its waveform becomes null in a resonant mode allowing the bridge switches to commutate under soft-switched condition. One example of a QSW inverter is shown in Fig. 8(a). It is claimed to produce less loss than other QSW topologies [10]. On the other hand, the Auxiliary Resonant Commutated Pole (ARCP), Fig. 8(b), has one auxiliary circuit per leg (local commutation). This inverter has been shown to produce fewer losses among a number of examined soft-switched topologies with local commutation [11]. However, it is also less efficient than the hard-switched inverter for a switching frequency up to 10 kHz [12].

The validity of the proposed technique was verified by

TABLE II
Application Example 1

Conditions: $E = 200V, R = 7.4\Omega, I_{\max} = 27A, m = 1, pf = 0.99, f_s = 20kHz$

PWM	Practical	Simulation with T effect	Simulation without T effect
SPWM	95.6 %	97.0 %	97.7 %
CPWM	95.8 %	96.7 %	97.4 %
DPWM1	95.8 %	96.7 %	97.5 %
DPWM2	96.4 %	97.9 %	98.3 %

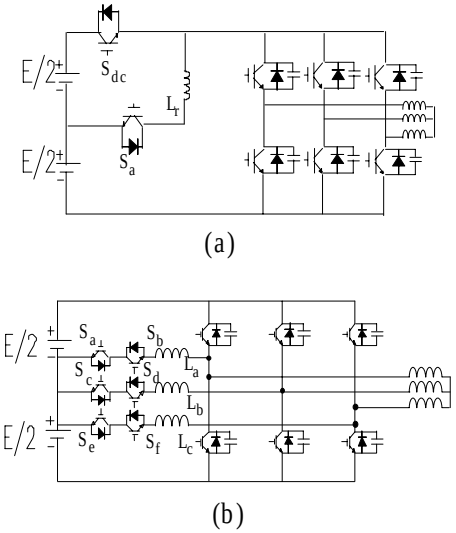

Fig.8. Examples of voltage inverters: (a) QSW and (b) ARCP

measurement of losses in the equivalent circuit (one phase-leg) of the QSW inverter in Fig. 8(a). In Fig. 9 the calculated efficiency is compared to the experimental efficiency of the QSW inverter. To obtain these results a dc load (R=11Ω, L=0.5mH) was used and the power changed from 225W (50V, 4.5A) to 5625W (250V, 22.5A). Note that the maximum error between the experimental results and the simulated results using the proposed equations is about 0.6%. This validates the technique since the errors are small. Note, also, that the largest error occurs for low power.

Figure 10 compares the losses of the hard-switched, ARCP and QSW inverters, at 150A when the frequency varies from 10 kHz to 50 kHz. All of them are fed from a voltage source of 500 V, use 20 kHz IGBT's, and supply a three-phase *R-L* load with a power factor of approximately 0.866. The current *I* refers to the maximum value of the sinusoidal current in the inverter output.

All topologies have been considered to operate with a PWM technique that takes into account the load phase angle [13]. A simulation program has been developed including the loss models of devices and taking into account he PWM strat-

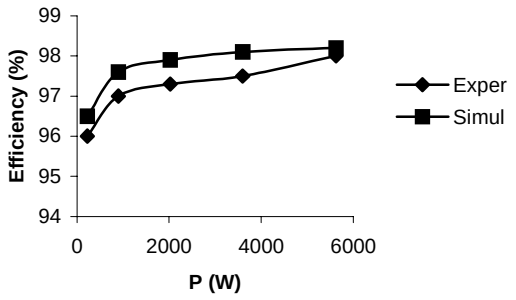

Fig.9. Comparison of experimental and calculated efficiencies for the QSW inverter in Fig. 8

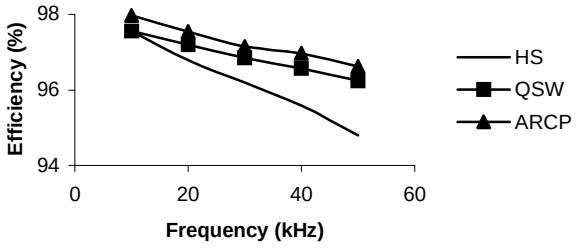

Fig.10. Comparison of efficiency in HS, ARCP, and QSW inverters with IGBT operating at E=500V and I=150A

egy. Such a program is basically that used to digitally control the converter in practice.

The results in Fig. 10 favor the ARCP inverter in the frequency range examined. The efficiency of the QSW inverter is close to that of the ARCP inverter, the 0.4% difference being is mainly due to the losses in S_{dc}. The HS inverter presents the worst results and deteriorates as the frequency of operation increases.

IV. CONCLUSION

The objective of this paper is to propose a method of losses estimation for any application using IGBT. The proposed models help designers to choose an IGBT for specific conditions regardless the conditions specified in the device data sheet. The models are based on experimental results carried out with simple circuits to measure conduction and switching losses for the chosen device. By changing conditions, the user can get enough data to build models and estimate losses for his specific application. The models are shown to be efficient for estimation of IGBT losses at operating points that are different from those indicated in data sheets, inclusive when the IGBT operates under soft switching conditions.

ACKNOWLEDGEMENT

Authors would like to acknowledge the Conselho Nacional de Pesquisas e Desenvolvimento (CNPq) for its support of this work.

REFERENCES

[1] F. Blaabjerg, U. Jaeger, S. Nielsen, and J. Pedersen, “Power Losses in PWM-VSI Inverter using NPT or PT IGBT Devices”, *in Proc. PESC Rec.*, pp. 434-441, 1994.

[2] S. Clemente and B. Pelly, “An Algorithm for the Selection of the Optimum Power Device for the Electrical Vehicle Propulsion”, *in Workshop on Power Electronics in Transportation*, pp. 129-136, 1992.

[3] J. Kolar, H. Ertl, and F. Zach, “Influence of the Modulation Method on the Conduction and Switching Losses of a PWM Converter System”, *IEEE Transactions on Industry Applications*, vol. 27, no. 6, pp. 1063-1075, 1991.

[4] L. Mestha and P. Evans, “Analysis of On-State Losses in PWM Inverters” IEE Proceedings, Vol. 136, No. 4, 1989, pp. 189-195.

[5] J.S. Lai, R.W. Young, and J.W. McKeaver, “Efficiency consideration of DC link soft-switching inverters for motor applications,” in *Proceedings of the IEEE PESC*, 1994, pp. 1003-1010.

[6] K.M. Smith and K.M. Smedley, “A comparison of voltage mode soft switching methods for PWM converters,” in *Proceedings of The IEEE APEC*, 1996, pp. 291-298.

[7] F.T. Wakabayashi and C.A. Canesin, “A new HPF-PWM boost rectifier,” in *Proceedings of the* COBEP (Brazilian Conference on Power Electronics), 1999, pp. 417-422.

[8] T.S. Wu, M.D. Bellar, A. Tchamdjou, J. Mahdavi, M. Ehsani, "A review of soft-switched DC-AC converters", IEEE IAS'1996 Conference Record, 1996, pp. 1133-1144.

[9] H.W. van der Broeck and H.C. Skudelny and G.V. Stanke, "Analysis and realization of a pulsewidth modulator based on voltage space vectors", *IEEE Transactions on Industrial Applications*, Vol. 24, No. 1, 1988, pp. 142-150.

[10] M.C. Cavalcanti, E.R. da Silva, and C.B. Jacobina, “An improved quasi-square-wave DC-link converter,” in *Proceedings of the IEEE IAS*, 2002, pp. 2320-2326.

[11] J.S. Lai, R.W. Young, and J.W. McKeaver, "Efficiency Consideration of DC Link Soft-Switching Inverters for Motor Applications", IEEE PESC'94 Conference Record, 1994, pp. 1003-1010.

[12] W. Dong, J., Y. Choi, Y. Li, D. Boroyevich, F.C. Lee, J. Lai, and S. Hitti, "Comparative experimental evaluation of soft-switching inverter techniques for electric vehicle drive applications", in IEEE IAS Conf. Rec., 2001, CD 01CH37248C.

[13] M.C. Cavalcanti, E.R. da Silva, A.M.N. Lima, C.B. Jacobina, and R.N. Alves, “Reducing losses in three-phase PWM pulsed dc-link voltage type inverters systems,” *IEEE Transactions on Ind. Applications*, v. 38, n. 4, Jul./Aug., 2002, pp. 1114-1122.